Available online at www.sciencedirect.com
ScienceDirect
Journal of the European Ceramic Society 30 (2010) 3235–3243
www.elsevier.com/locate/jeurceramsoc

# Electrochemical studies of carbon-rich polymer-derived SiCN ceramics as anode materials for lithium-ion batteries

Magdalena Graczyk-Zajac, Gabriela Mera, Jan Kaspar, Ralf Riedel *

*Technische Universität Darmstadt, Institut für Materialwissenschaft, Petersenstrasse 23, D-64287 Darmstadt, Deutschland, Germany*

Received 12 April 2010; received in revised form 14 June 2010; accepted 1 July 2010
Available online 31 July 2010

**Abstract**

The electrochemical behavior of poly(phenylvinylsilylcarbodiimide)-derived SiCN ceramics as anode material for lithium-ion batteries is reported here for the first time. The novel carbon-rich silicon carbonitride (SiCN) ceramics have been synthesized by the thermal treatment of poly(phenylvinylsilylcarbodiimide) under argon atmosphere at five temperatures, namely 1100, 1300, 1500, 1700 and 2000 °C. The SiCN electrodes were prepared without any conducting additives and were tested in electrochemical two electrodes cell using cyclic voltammetry and galvanostatic techniques. The capacity of the carbon-rich SiCN samples was found to be stable upon galvanostatic cycling and reaches almost 300 mAh/g for the sample prepared at 1300 °C with oxygen as the impurity. The dependence of the microstructure, especially of the crystallinity of the segregated carbon phase and of the oxygen impurities on the electrochemical behavior of the SiCN material, was analysed. At all temperatures of thermolysis, the free carbon phase has been identified as "soft carbon".


*Keywords:* Li-ion batteries; Anode; SiCN ceramic; Polymer-derived ceramic; Soft carbon

## 1. Introduction

The increase in energy density and power density requirements for lithium-ion batteries leads to continuous research for new electrode materials. Various insertion materials have been proposed as negative electrodes for rechargeable batteries.[1–3] The highest theoretical capacity is obtained when using metallic lithium (3862 mAh/g) or elemental silicon forming lithium-rich alloys (3578 mAh/g).[4] However these materials are not commercialized yet due to safety reasons and rapid capacity fading.

Currently available carbonaceous materials for lithium-ion batteries belong to two major classes, namely graphitic and non-graphitic (disordered) carbons.[5] Graphitic materials have been extensively studied[1,6] as mostly commercial graphite is used due to its low price and high reversibility despite its relatively low capacity (372 mAh/g). Less attention has been paid to lithium insertion into disordered carbons even though these carbons may find attractive applications as anodes for two general reasons: (1) by varying the synthesis temperature (typically, materials preparation involves pyrolysis of an organic carbon-containing polymer or hydrocarbon molecules) and the nature of the carbon precursor, it is possible to tailor the final electrochemical properties; (2) Some of these materials demonstrate high reversible capacity in the range of 400–1000 mAh/g.[7] Lithium intercalation in some disordered carbons derived from various precursors, e.g. sucrose,[8,9] petroleum coke,[10] pitch-polysilanes blends,[11,12] siloxanes,[13–18] and silazanes[19–22] has been studied in the presence of conductive additives such as acetylene black powder.[22] It was demonstrated that despite the quite high irreversible capacity observed during first intercalation/deintercalation, the disordered carbons are perspective materials for negative electrodes in lithium-ion batteries because of their relatively high reversible capacity, stability in cycling, low price and availability. Polymer-derived SiCN ceramics have several properties which make them promising to be used as electrode material in Li-ion batteries. These polymer-derived ceramics (PDCs) are chemically inert towards battery components, can minimize the agglomeration of lithium and are light weight materials.[19] Graphite anodes suffer from structural degradation by means of exfoliation due to repeated insertion of lithium into the graphene

* Corresponding author. Tel.: +49 6151 166347; fax: +49 6151 166346.
*E-mail address:* riedel@materials.tu-darmstadt.de (R. Riedel).

0955-2219/$ – see front matter © 2010 Elsevier Ltd. All rights reserved.
doi:10.1016/j.jeurceramsoc.2010.07.010

layers. Polymer-derived SiCN ceramic electrodes could be an alternative in order to avoid this problem. Furthermore, PDCs properties can be designed by varying the starting polymer composition. The preceramic polymers can provide a ceramic with a high excess of carbon ($C_{free}$). This carbon forms a continuous network for the storage of lithium-ions.[17,18] The presence of carbon embedded in a silicon-based matrix make these materials more stable than free-standing carbon, for instance against oxidation. The amount of $C_{free}$ is also tuned by the design of the preceramic polymers. Generally, silicon polymers containing phenyl substituents at silicon provide a high amount of free carbon in the ceramic by means of thermal decomposition in an inert atmosphere.

Kolb et al. discovered in 2006[20] that pure polyvinylsilazane-derived SiCN ceramic electrodes prepared without any conductive additives show a low electrochemical activity, namely a discharge capacity between 4 and 39 mAh/g depending on the final temperature of thermolysis. The aim of the present study now is to demonstrate the synthesis of SiCN ceramics with higher carbon content and significantly enhanced electrochemical properties suitable for anode materials in lithium-ion batteries.

## 2. Experimental part

### 2.1. Synthesis

The poly(phenylvinylsilylcarbodiimide) polymer was synthesized as reported in Ref. [20] by the reaction of phenylvinyldichlorosilane with stoichiometric amounts of bis(trimethylsilylcarbodiimide). For the thermolysis of the sample at 1100 °C, 2 g of the preceramic polymer was filled in a quartz crucible. The crucible was then put in a quartz tube, evacuated, subsequently filled with Ar gas and finally heated under a steady flow of purified argon (50 mL/min) in a programmable horizontal tube furnace with a heating rate of 100 °C/h. For the thermolysis at higher temperatures (1300 and 1500 °C), the samples were pyrolyzed at 1100 °C in a first step following the procedure described above and then heated with 100 °C/h in a SiC crucible in a programmable horizontal furnace. For the thermolysis at 1700 and 2000 °C, 0.5 g of the SiCN ceramic synthesized at 1100 °C was annealed in a resistively heated Astro furnace with a heating ramp of 5 °C/min to the required pyrolysis temperature. For all the experiments, the dwelling time was 2 h. The thermolysis was completed by cooling the samples to room temperature with a cooling ramp of 1.66 °C/min for the experiments at 1100, 1300 and 1500 °C and with a ramp of 10 °C/min for the experiments performed at 1700 and 2000 °C. The pyrolysis of the sample 2_O with oxygen contamination was performed without evacuation of the quartz tube before starting the experiment.

### 2.2. Preparation of material and electrodes

Prior to electrode preparation each powder was "hand-ground" for 15 min. Then the material was mixed with 10 wt.% polyvinylidene fluoride (PVdF, SOLEF) solution in N-methyl-2-pyrrolidone (NMP, BASF). The ratio active material/PVdF was 9:1 and was constant for all the samples. NMP was added in order to form homogeneous slurry (about 0.8 g of solvent for 1 g of solution). The slurry was spread on the rough side of a copper foil (10 μm, Copper SE-Cu58 (C103), hard as rolled Cu-treatment on one side, one side shiny Schlenk Metallfolien GmbH & Co KG) using a hand blade coating technique and dried at 80 °C for 24 h. The active material loading was always between 3 and 4 mg/cm$^2$. After drying, thin cylinders (electrodes) of 10 mm in diameter were cut and some of them were pressed with 75 kN/cm$^2$ during 3 min. The weight of electrodes was measured, and then the electrodes were dried under vacuum at 90 °C for 48 h in a Buchi oven and transferred directly into the glove box (MBraun Glove Box Systems, $H_2O$, $O_2$ <1 ppm) without contact with air.

### 2.3. Characterization techniques

All the electrochemical measurements were performed in two electrodes Swagelok® type cells, with active material as working electrode and lithium foil (99.9% purity, 0.75 mm thick, Alfa Asear) was used as counter/reference electrode. High purity solution of 1 M $LiPF_6$ in ethylene carbonate (EC) and dimethylcarbonate 1:1 (LP30, Merck KGaA) was used as electrolyte. Porous polypropylene membrane (Celgard 2500) was used as separator.

Hermetically closed cells were electrochemically tested by means of galvanostatic and cyclic voltammetry (CV) methods using a VMP multipotentiostat (BioLogic Science Instruments).

The crystallinity of the samples was investigated by powder X-ray diffraction measured by a STOE X-ray diffractometer using Ni-filtered Cu $K_\alpha$ radiation at a scan speed of 1° min$^{-1}$.

For the chemical analysis of the ceramics, the carbon content was determined by a carbon analyser (CS 800, Eltra GmbH, Neuss). The oxygen and nitrogen contents of the powdered ceramic sample were measured by a N/O analyser (Leco, Type TC-436).

Raman spectra were recorded on a confocal Horiba HR800 micro-Raman spectrometer using an excitation laser wavelength of 514.5 nm. For the evaluation of free carbon cluster size in ceramics, a Gaussian–Lorentzian curve fitting of the Raman bands (LabSpec 5.21.08 Software) was applied.

## 3. Results and discussion

Carbon-rich SiCN ceramics are a new class of nanostructured ceramics having interesting physical properties such as electrical conductivity and high resistance against crystallization. This particular property profile is basically related to the significant amount of carbon in the SiCN microstructure.[23] Due to the high carbon content of poly(phenylvinylsilylcarbodiimide) derived SiCN phases in the order of 48–76 wt.% we were interested to study their electrochemical performance and to evaluate their potential application as alternative anode material in lithium-ion battery.

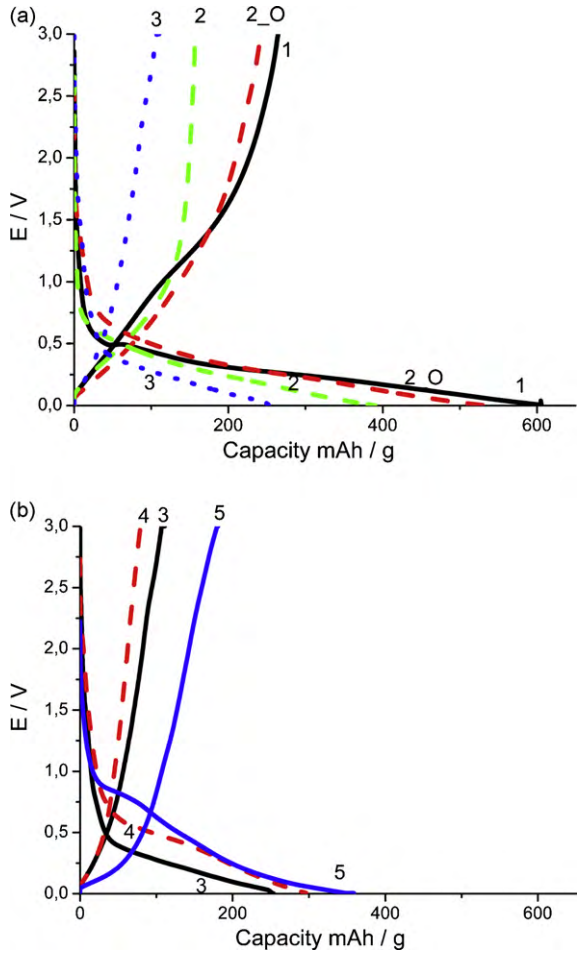


Fig. 1. First lithium intercalation/deintercalation cycle for samples 1–3 (a) and 3–5 (b). Rate of charging/discharging: C/20, D/20.

### 3.1. Electrochemical studies: first lithium intercalation/extraction

Fig. 1 presents the first galvanostatic intercalation/deintercalation cycle of the SiCN ceramic synthesized at (a) 1100 °C (sample 1), 1300 °C (sample 2), 1300 °C with oxygen impurities (sample 2_O), 1500 °C (sample 3) and (b) 1500 °C (sample 4), 1700 °C (sample 5), and 2000 °C (sample 6). The data, corresponding to capacity values obtained during the first charge/discharge and capacity losses, i.e. irreversible capacity, are summarized in Table 1. The efficiency, $\eta$, is calculated as the ratio of the first discharge (deintercalation) capacity to the first charge (intercalation) capacity, namely $C_{discharge}/C_{charge}*100\%$. This value enables an estimation of the quantity of charge captured irreversibly during the first cycle.

For the samples prepared at lower temperatures (samples 1 and 2), an unusual high capacity of the first charge is observed. Charging transients for the samples 1–3 have a similar shape, the electrochemical process starts at a potential lower than 0.6 V. Charge losses related to the insertion of solvated lithium, $Li_x(solv)_yC_6$ (0.5–1 V interval), capacity losses related to the formation of a passivating layer of the solid electrolyte interface (SEI), usually visible at around 1–1.2 V, are not observed for the studied SiCN ceramics. The insertion of $Li_x(solv)_yC_6$ and charge losses caused by this process starts to appear for sample 4 and are well visible for sample 5. This phenomenon is discussed in more detail together with the analysis of the cyclic voltamperommetry curves.

The samples 1 and 2_O demonstrate the highest reversible capacity of more than 200 mAh/g. The significant difference can be noticed between sample 2 and 2_O in the capacity of first charge/discharge. The shape of the charging curves for both materials is similar however discharging transients are only similar for potentials lower than 1.3 V. Up to this potential sample 2 is practically discharged. Sample 2_O recovers a significant part of discharge capacity at potentials higher than 1.3 V. The behavior of sample 2_O resembles more that of sample 1, while the discharge curve of sample 2 is similar to that of sample 3.

Increasing the pyrolysis temperature up to 1500 °C, the capacity of the first charge and discharge decreases with efficiency remaining almost stable (43–48%). This finding can be considered as a typical electrochemical behavior of disordered carbons. Non-graphitic, disordered carbons are mostly prepared by precursor pyrolysis at temperatures below ~1500 °C. Heat-treatment at temperatures from ~1700 to ~2000 °C allows it to distinguish between two different carbon types, namely a non-graphitizing disordered carbon phase and a turbostratic C-phase (see Fig. 2).

Graphitizing carbons develop graphite continuously during the heating process, as stacking between the carbon layers is weak and, therefore, the layers are mobile enough to form graphite-like crystallites. Non-graphitizing carbons show no true development of the graphite structure even at high temperatures (2500–3000 °C), as the carbon layers are immobilized by cross-linking between the layers. Since non-graphitizing carbons are mechanically harder than graphitizing ones, it is common to subdivide the non-graphitic carbons into "soft" and "hard"

Table 1
Capacity values of the first galvanostatic lithium intercalation/deintercalation (data taken from Fig. 1). Efficiency calculated as $C_{discharge}/C_{charge}*100\%$, $C_{irr} = C_{charge} - C_{discharge}$.

| Sample | $T_{thermolysis}$ (°C) | $C_{charge}$ (mAh g$^{-1}$) | $C_{discharge}$ (mAh g$^{-1}$) | $C_{irr}$ (mAh g$^{-1}$) | $\eta$ (%) |
|---|---|---|---|---|---|
| 1 | 1100 | 605 | 263 | 342 | 43 |
| 2 | 1300 | 365 | 176 | 189 | 48 |
| 2_O | 1300 | 532 | 241(~290[a]) | 291 | 45 |
| 3 | 1500 | 253 | 108 | 145 | 43 |
| 4 | 1700 | 300 | 80 | 220 | 27 |
| 5 | 2000 | 360 | 180 | 180 | 50 |

[a] The capacity obtained after 120 cycles.

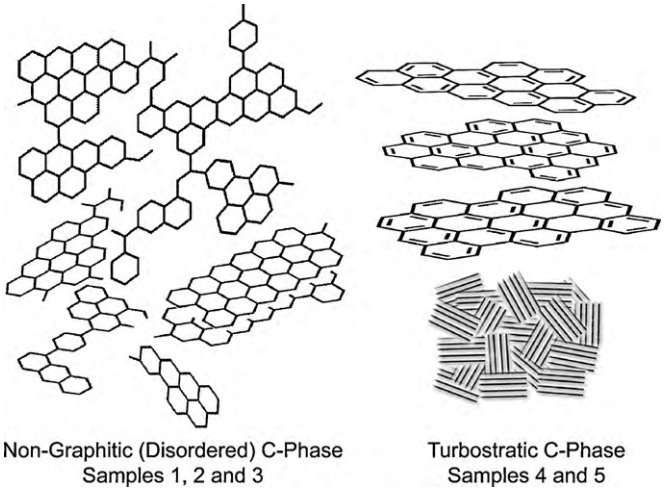


Fig. 2. Carbon fate in poly(phenylvinylsilylcarbodiimide)-derived SiCN ceramics in dependence of the temperature of thermolysis.

carbons.[24] Many types of carbon contain both graphitic and non-graphitic structural units, which makes the classification into graphitic and non-graphitic types sometimes arbitrary. Usually "soft" carbons consist of graphene layers which can develop graphitic structures with increasing temperature.[6] In numerous studies related to disordered carbons, Dahn et al.[7–14,25,26] have demonstrated that in both cases, for soft and hard carbons, the reversible capacity reaches its minimum for heat-treatments of the materials at about 1700 °C. However the reversible capacity of hard carbons thermolyzed at $T < 1700$ °C should be higher than that observed for our SiCN samples 1, 2 and 3. This result indicates the presence of soft disordered carbons in our investigated materials. This finding is an important result as until now, there are no reports on the electrochemical nature of the free carbon phase in polymer-derived SiCN ceramics. As in the case of soft carbons, a significant increase of the reversible capacity can be noticed for the sample prepared at 2000 °C.

Fig. 3 demonstrates the first (a) and second (b) voltammetry cycles for samples 1, 3, and 5. With increase of the pyrolysis temperature (sample 1 to sample 5), one can easily notice the evolution of the shape of the cyclic voltammetry (CV) curves. Let us start with the analysis of the cathodic branch: lithium intercalation into the electrode. For SiCN prepared at lower temperatures (samples 1 and 3), the electrochemical process (charge passing) during the first cycle starts only at a potential lower than 0.5–0.6 V. At those potentials one can expect the intercalation of non-solvated lithium inside a carbonaceous structure. The insertion of solvated lithium ($Li_x(solv)_yC_6$), usually occurring between 0.5 and 1 V, was not identified in our system. This behavior is an advantageous feature as insertion of solvated lithium is the main reason of exfoliation and high irreversible capacity losses.[27] Moreover, this is another typical feature of "soft" carbons (e.g. turbostratic carbons containing some disordered carbon "contaminations") where the cross-linking of graphene layers can mechanically suppress the formation of $Li_x(solv)_yC_6$.[1,27]

Capacity losses related to the formation of a passivating layer of solid electrolyte interface (SEI), usually visible at about 1–1.2 V, were not found for the studied SiCN ceramics. With increasing of the annealing temperature (samples 4 and 5, see also galvanostatic charging/discharging in Fig. 1b), it can be seen that an electrochemical reaction at the carbon surface starts close to 1 V. This behavior is already pronounced for sample 4 and clearly evident for sample 5. The irreversible charge has to be attributed to the reaction of the electrolyte with the carbon surface. The shape of the cathodic branch of the CV for sample 5 is similar to that observed for graphitic materials.[27,28]

In the case of the anodic branch of the cyclic voltammetry curve (Fig. 3), it can be noticed that with increase of the thermolysis temperature, a peak evolution during lithium desinsertion at the potential lower than 0.5 V is distinguished. The CV curve for lithium deintercalation for sample 1 displays practically no peaks and an almost stable discharging current is observed in the measured potential range. For samples 3 and 5 almost no lithium is deintercalated after passing 0.5 V. This feature is also characteristic for graphitic carbons. It should be pointed out that after annealing of SiCN ceramic at 2000 °C we are not expecting the formation of a pure graphite phase (sample should be heated beyond 2000 °C); however we can already find quite regular arrangement of graphene sheets. The presence of turbostratic carbon (two dimensional randomly stacked graphene sheets, see Fig. 2) in poly(phenylvinylsilylcarbodiimide) derived

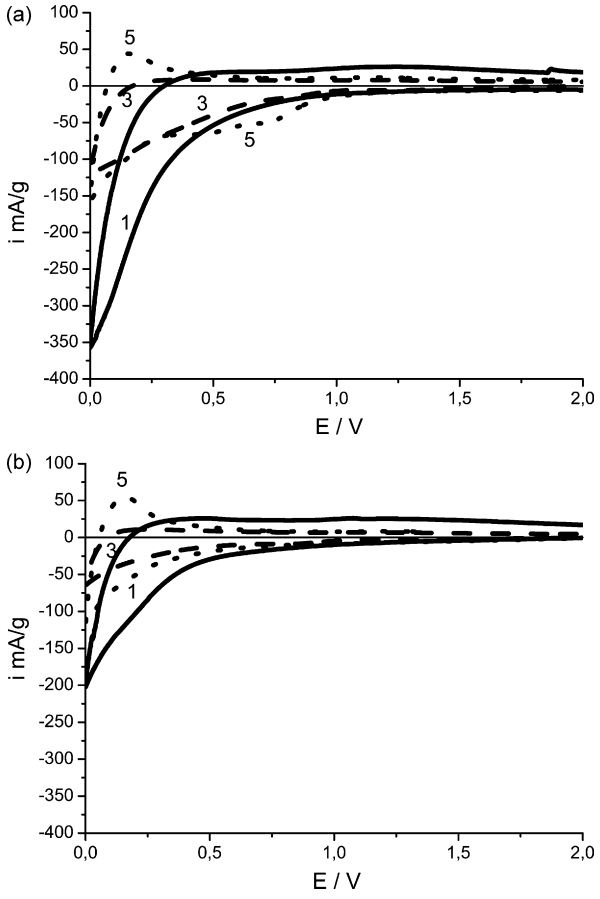


Fig. 3. Comparison of the first (a) and second (b) cyclic voltammetry cycle for the samples 1, 3 and 5; scan rate 50 μV/s between 0 and 3 V. Solid line: sample 1, dashed line: sample 3, dotted line: sample 5.

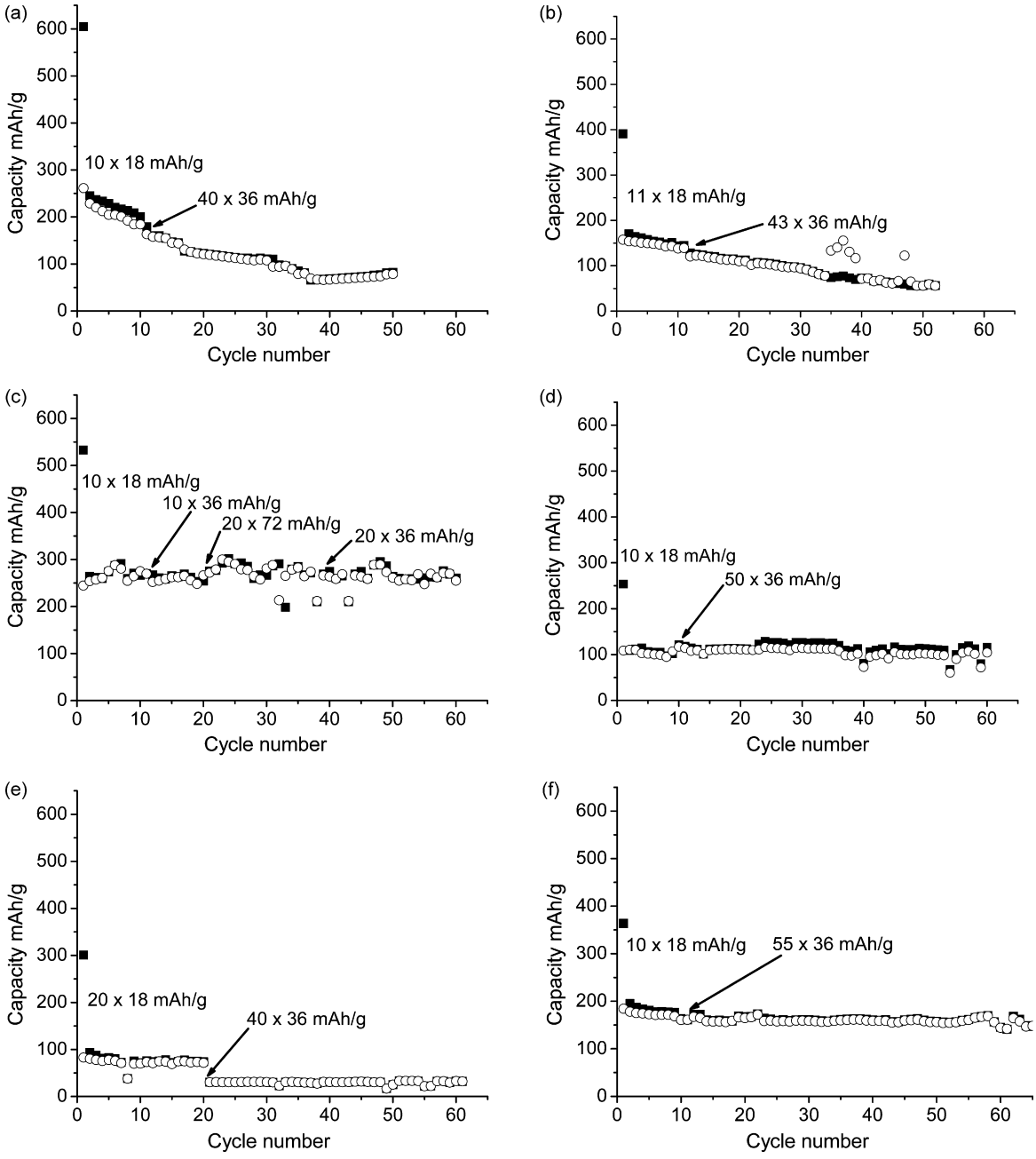


Fig. 4. Cycling behavior (capacity vs cycle number) of samples 1 (a), 2 (b), 2_O (c), 3 (d), 4 (e) and 5 (f) in two-electrode cells. The number of complete charging/discharging cycles and applied current is indicated inside each figure, i.e. 10 mAh/g × 20 mAh/g means that that the cell was ten times charged and discharged with 20 mA per gram of active material used. Arrow indicates the cycle with increasing current, charge (filled squares), discharge (open dots).

SiCN heat-treated at 2000 °C has been already proved by X-ray diffraction as discussed in reference.[23] In this study we can also find that starting from 1500 °C, a β-SiC phase begins to develop. The presence of this phase will decrease the overall materials reversible and irreversible capacity, since it is not active in the lithium insertion/deinsertion process.[29] This finding explains the relatively low reversible capacity of 80–180 mAh/g measured for samples 3–5, instead of about 300 mAh/g expected for turbostratic (or pre-turbostratic) carbons.[30]

The highest discharge capacities are observed for samples 1 and 2_O, namely 263 and 241 mAh/g, respectively. Such capacity values are characteristic for most of "soft" carbons heated beyond 1100 °C.[7] However, the high reversible capacities are accompanied by high irreversibility. There are two possible explanations of this phenomenon based on an interlayer distance model, presented by Azuma et al.[30] and the "house of cards" model developed by Dahn's group.[31] Both theories are related to the Franklin's model,[24] however the Azuma model was developed for the case of "soft" carbons and is, therefore, appropriate to explain the electrochemical behavior of the studied SiCN ceramics. According to calculations, based on $^{7}$Li NMR, lithium in soft organized carbon is in an almost fully ionic state and the carbon atom can receive at maximum 1/7.5 electrons while in graphite it can attain almost 1/6 electrons ($LiC_6$).

Therefore it is clear that we cannot expect more than 300 mAh/g of reversible capacity in samples 1 and 2. Franklin also showed[24] that regions of unorganized carbon, consisting of buckled single graphene layers or of tetrahedrally bonded carbon, separate the organized regions. In these regions lithium can be captured irreversibly and it can lead to high irreversible capacity.

The capacity of the studied samples diminishes with the increase of thermolysis temperature and reaches the minimum for sample 4 prepared at 1700 °C. We have already mentioned that such behavior is typical for "soft" carbons; however it does not explain such a significant difference between sample 3 and sample 4. In both cases a reversible capacity of ~150 mAh/g could be expected.[7] This feature can be explained considering that starting from 1500 °C, separation of a β-SiC phase from the SiCN matrix occurs. Due to this fact, a part of the electrochemically active mass is lost for lithium-ion insertion and the overall capacity diminishes with the thermolysis temperature, i.e. with the formation of inactive amount of SiC phase. The capacity again increases for the sample synthesized at 2000 °C because of crystallization of amorphous C as turbostratic carbon (see XRD analysis in Fig. 5b).

### 3.2. Extended cycling electrochemical behavior

Fig. 4a–f presents the extended cycling behavior of samples 1–5. All the samples demonstrate irreversible losses after the first intercalation, and with further cycling, a capacity coulombic efficiency of 100% can be noticed. A negligible incoherence can be found for sample 1 at the beginning of the cycling and for sample 2 after 30 cycles, but we cannot attribute it to any specific feature of those samples.

For each sample, two charging rates were used in order to investigate the fast cycling stability. For sample 2_O a higher current (corresponding to ~C/5, D/5 rate) was applied because of its exceptional stability and capacity increase during cycling. It can be noticed that the starting capacity of sample 1 is indeed the highest one; however it reduces with longer cycling. This material is also sensitive in the case the cell is charged/discharged with a higher current and as a result, the recovered capacity reduces to more than 50%. A similar performance is observed for sample 2. In contrary, sample 2_O pyrolyzed at 1300 °C (Fig. 4c) demonstrates an excellent stability during cycling, without capacity loss even if the applied current is five times higher than the initial one. During cycling, the overall capacity increases about 15% with respect to the first discharge capacity, remaining 280–290 mAh/g at the end of the measurement. No capacity diminution can be noticed when the applied current is increased. The capacity of sample 3 also remains stable by ~100 mAh/g. For sample 4 <100 mAh/g is recovered and the material is sensitive towards higher current. If the current is doubled, the capacity reduces almost 4 times and only ~20 mAh/g is recovered. This sample demonstrates also the most significant irreversible capacity losses and the calculated efficiency (Table 1) reaches only 27%. In contrary, sample 5 reveals the highest first cycle efficiency (50%) and a stable capacity (~200 mAh/g), not affected by the increase of the applied galvanostatic current.

Table 2
Elemental composition of samples 1–5. The amount of silicon is calculated as the difference to 100% assuming that we have less than 1 wt.% of H in the composition.

| Sample | $T_{thermolysis}$ (°C) | C (wt.%) | N (wt.%) | Si (wt.%) | O (wt.%) |
|---|---|---|---|---|---|
| 1 | 1100 | 55.60 | 14.20 | 25.40 | 4.80 |
| 2 | 1300 | 50.95 | 14.93 | 31.84 | 2.28 |
| 2_O | 1300 | 48.30 | 10.54 | 30.43 | 10.73 |
| 3 | 1500 | 69.75 | 6.55 | 23.21 | 0.49 |
| 4 | 1700 | 72.05 | 0.20 | 27.75 | 0.00 |
| 5 | 2000 | 76.27 | 0.04 | 23.69 | 0.00 |

In order to understand the extended cycling behavior of the studied samples, in particular the high capacity of sample 2_O, we correlate the electrochemical properties with the sample composition (Table 2) and their structural properties as reported in references.[23,32] A characteristic feature of the carbon-rich polysilylcarbodiimide-derived SiCN ceramics is the presence of several types of nanodomains in the microstructure. The ceramics contain nanodomains comprised of amorphous phases, a-$Si_3N_4$, a-SiC and a-C, up to 1500 °C at which SiC starts to crystallize in the ß-polymorph (see Figs. 5 and 6b). After annealing of the SiCN phase at 1700 °C, the carbon phase rearranges to form turbostratic type of carbon.

The presence of high amount of free carbon in the microstructure and its fine and homogeneous distribution (see Raman spectra, Fig. 6a) allows these ceramics to be electrically conductive. The lateral cluster size of carbon ($L_a$) was calculated to 1.23 up to 1.77 nm from the intensity of the D and G bands in the Raman spectra using the formula reported by Ferrari and Robertson[33]: $I(D)/I(G) = C'(\lambda)L_a^2$.

From 1100 to 1500 °C, the ceramics exhibit broad signals and a strong overlap as a consequence of the pronounced structural disorder of the carbon phase. Comparing the samples 2 and 2_O

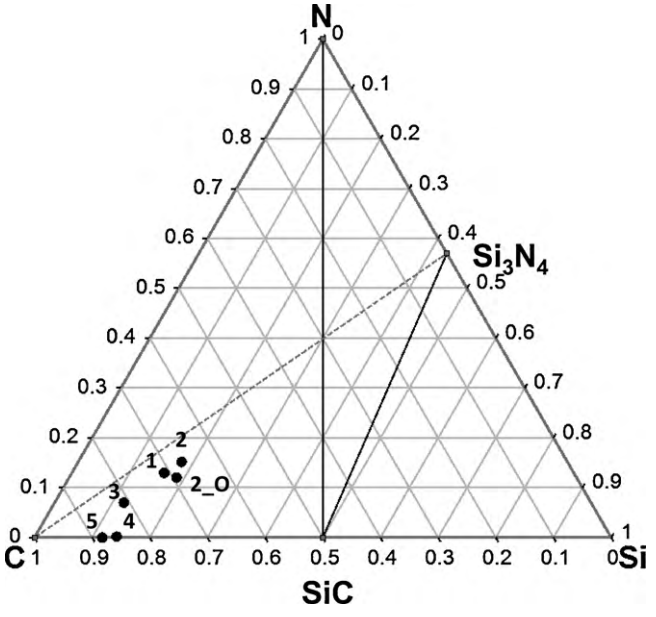


Fig. 5. Composition diagram of SiCN samples prepared at 1100, 1300, 1500, 1700 and 2000 °C (indicated as 1–5, respectively).

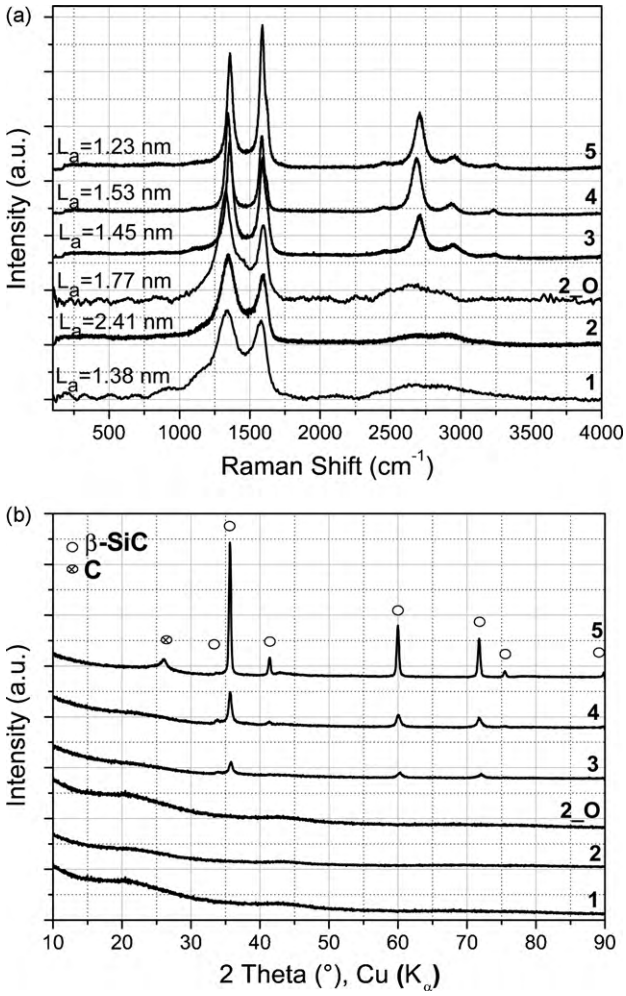


Fig. 6. Raman spectroscopy (a) and XRD (b) analysis of samples prepared at 1100, 1300, 1500, 1700 and 2000 °C under Ar.

synthesized at 1300 °C with and without significant amount of oxygen, respectively, it is interesting to analyse a difference in the carbon cluster size. The sample with 10.73 wt.% O shows a finer distribution of carbon due to a lower $L_a$ size. The decrease in $L_a$ cluster size can be associated with a higher activity versus Li intercalation. At 1700 °C, very distinct and narrow peaks of the D and G modes are found due to an enhanced ordered graphite-like structure (graphene layers). At 2000 °C, turbostratic carbon is formed, as indicated primarily by the increase in the intensity of the G band and the concomitant decrease of the D band as well as by the overtone band profile.

For samples 1–5 the carbon content increases gradually with increasing thermolysis temperature. The silicon content remains relatively constant and varies between 23 and 32 wt.% and the amount of oxygen decreases with increasing pyrolysis temperature. Due to the higher amount of oxygen in sample 2_O (more than 10 wt.%), the amount of carbon is lower with respect to the other analysed samples. However this sample presents the best electrochemical properties. A similar feature has been demonstrated for another group of SiCN materials.[20] Contrary, it has been also reported that the presence of oxygen, e.g. in pyrolysed pitch-polysilane blends[34] increases the irreversible capacity. Therefore, the presence of oxygen can explain to some extent the high irreversible capacity found in sample 2_O.

The nature of free carbon phase plays the most important role in the electrochemical behavior of carbon-rich SiCN ceramics and is strongly dependent on the composition and constitution of the preceramic polymer. From 1100 to 1500 °C we can discuss about the formation of disorded carbon and then, at 1700 and 2000 °C turbostratic carbon phases are formed. From an electrochemical point of view, at all these temperatures of thermolysis, we can identify the presence of soft carbons segregated from the SiCN phase. The evolution of specific capacity of soft carbons from 1000 to 2000 °C is well discussed in the literature, with values between 100 and 350 mAh/g and a minimum at 1700 °C [see Ref. [7 and references therein]]. A similar evolution of the capacity values is found also in the case of our investigated SiCN ceramics in this temperature interval. Fig. 7 presents the dependence of the reversible capacity on the final annealing temperature.

This finding leads to the conclusion that the amount of the segregated carbon and its nature determine the electrochemical activity of our SiCN ceramics. In the same time, the existence of silicon-based phases, namely amorphous $Si_3N_4$ and SiC from 1100 up to 1500 °C and the presence of crystalline SiC after annealing at 1700 and 2000 °C, increases the stability of the materials, for instance against oxidation.

In order to fully understand the irreversible losses found in the analysed materials one should take into account that our samples synthesized up to 1500 °C contain amorphous $Si_3N_4$ which starts to convert to inactive SiC phase beyond that temperature by means of a carbothermal reaction according to a-$Si_3N_4$ + 3a-C → 3β-SiC + 2 $N_2$. It has been found[35] that milled crystalline $Si_3N_4$ can insert Li with about 50% reversibility, the reversibility increasing with milling time, i.e. smaller $Si_3N_4$ particles result in higher charge/discharge material capacity. On the basis of our previous investigations we know that samples 1, 2 and 3 consist of amorphous nanostructured silicon nitride and we can attribute the additional capacity (irreversible as well as reversible) and stability to the presence of $Si_3N_4$. However, it is difficult to

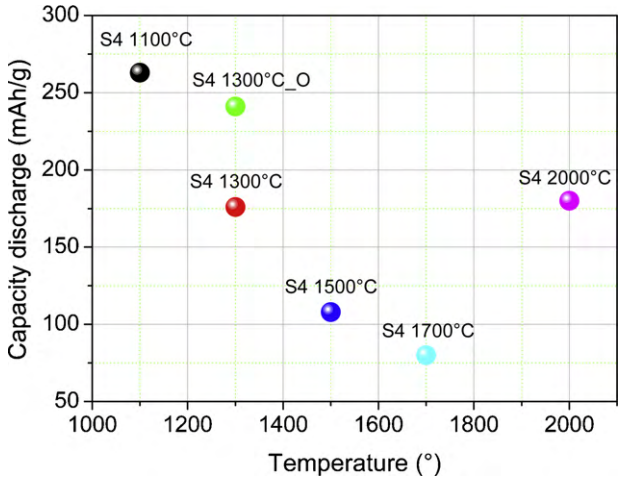


Fig. 7. Dependence of the reversible capacity on the processing temperature of samples 1–5.

distinguish the lithium insertion into disordered carbons from that into $Si_3N_4$ as the intercalation/deintercalation takes place at potentials similar to disordered carbons, i.e. between 1.5 and 0 V.

## 4. Conclusions

In this study we have analysed for the first time the electrochemical performance of carbon-rich poly(phenylvinylsilylcarbodiimide)-derived SiCN ceramic materials for application as anode material in lithium-ion batteries. Six samples were prepared in a wide range of temperatures, ranging from 1100 to 2000 °C and containing soft carbons as the free carbon phase. The annealed SiCN ceramics can be reversibly intercalated by lithium with a reversible capacity varying from 80 to 290 mAh/g. The electrochemical performance and stability of carbon-rich SiCN ceramics against galvanostatic charge/discharge process was investigated by extended cyclization of the samples. After the first charge/discharge, all the investigated samples show a coulombic efficiency of 100%. Increasing amount of electrochemically inactive β-SiC phase, developed at an annealing temperature of 1500 °C and higher is found to be responsible for lower capacity values of samples prepared at 1500, 1700 and 2000 °C. The evolution of capacity, depending on the temperature of thermolysis, was found to be quite similar to that of soft carbons as reported in the literature. In polymer-derived SiCN ceramics, the soft carbon phase is embedded in a matrix of silicon-containing phases, which protects the carbon phase from oxidation or other corrosion phenomena.

The sample prepared at 1300 °C in the presence of air (sample 2_O) demonstrates the highest reversible capacity (290 mAh/g) and an enhanced cycling stability. The presence of ca. 10 wt.% of oxygen in the solid phase structure leads to a broader discharging potential interval. Sample 2 can be completely discharged up to 1.3 V while for sample 2_O, a significant part of charge is recovered at the potentials between 1.3–3 V having a behavior similar to that of sample 1. Further studies are required in order to understand the influence of oxygen on the electrochemical performance of our analysed materials. The high capacity of sample 2_O can be assigned to the presence of a high content of disordered carbon and the presence of oxygen in the SiCN phase. More details of the electrochemical behavior of carbon-rich SiCN ceramics and their dependence on the presence of oxygen are currently under investigation and will be published in a separate paper. Additionally, sample 2_O exhibits no significant capacity variation by increasing the charge/discharge current. This feature is important for materials used for "high power" application in batteries, e.g. for electric vehicles.

In conclusion, the composition and structure of PDCs can be easily tuned by changing the precursor chemistry and processing conditions. The dependence of the electrochemical properties of carbon-rich SiCN ceramics on their composition and structure demonstrate the advantage of the chemical design in order to improve the electrochemical performance. Several polysilylcarbodiimide-derived ceramics with even higher carbon content than that investigated in this study are currently under investigation and will be published in a following paper.

## Acknowledgments

This study was performed within the collaborative research center SFB 595/A4 funded by the Deutsche Forschungsgemeinschaft (DFG), Bonn, Germany and within the DFG-NSF research initiative "Stability of the NanoDomain Structure of Polymer-Derived SiCN Ceramics at High Temperatures". We gratefully acknowledge also the financial support by the Fonds der Chemischen Industrie, Frankfurt (Germany). Moreover, the authors want to thank H. Nguyen and Dr. A.P. Nowak for the assistance in performing part of the synthesis and electrochemical experiments.

## References

1. Winter M, Besenhard JO, Spahr ME, Novák P. Insertion electrode materials for rechargeable lithium batteries. *Adv Mater* 1998;**10**:725–63.
2. Bruce PG, Scrosati B, Tarascon JM. Nanomaterialien für wiederaufladbare Lithiumbatterien. *Angew Chem Int Ed* 2008;**47**:2930–46.
3. Kasavajjula U, Wang C, Appleby AJ. Nano- and bulk-silicon-based insertion anodes for lithium-ion secondary cells. *J Power Sources* 2007;**163**:1003–39.
4. Obrovac MN, Christensen L. Structural changes in silicon anodes during lithium insertion/extraction. *Electrochem Solid State Lett* 2004;**7**:A93–6.
5. Kinoshita K. Carbons. In: Besenhard JO, editor. *Handbook of battery materials*. Weinheim, Germany: Wiley–VCH; 1999. p. 231–44.
6. Winter M, Besenhard JO. Lithiated carbons. In: Besenhard JO, editor. *Handbook of battery materials*. Weinheim, Germany: Wiley–VCH; 1999. p. 383–418.
7. Dahn JR, Zheng T, Liu Y, Xue JS. Mechanisms for lithium insertion in carbonaceous materials. *Science* 1995;**270**:590–3.
8. Buiel E, George AE, Dahn JR. On the reduction of lithium insertion capacity in hard-carbon anode materials with increasing heat-treatment temperature. *J Electrochem Soc* 1998;**145**:2252–7.
9. Buiel E, Dahn JR. Li-insertion in hard carbon anode materials for Li-ion batteries. *Electrochim Acta* 1999;**45**:121–30.
10. Jean M, Desnoyer C, Tranchant A, Messina R. Electrochemical and structural studies of petroleum coke in carbonate-based electrolytes. *J Electrochem Soc* 1995;**142**:2122–5.
11. Xing W, Wilson AM, Zank G, Dahn JR. Pyrolyzed pitch-polysilane blends for use as anode materials in lithium ion batteries. *Solid State Ionics* 1997;**93**:239–44.
12. Dahn JR, Wilson AM, Xing W, Zank GA, inventors. Dow Corning Corp., assignee. Method of forming electrodes for lithium ion batteries using polycarbosilanes. United States patent US 5,907,899; 1999, Jun 1.
13. Xing W, Wilson AM, Eguchi K, Zank G, Dahn JR. Pyrolyzed polysiloxanes for use as anode materials in lithium-ion batteries. *J Electrochem Soc* 1997;**144**:2410–6.
14. Wilson AM, Zank G, Eguchi K, Xing W, Dahn JR. Pyrolysed silicon-containing polymers as high capacity anodes for lithium-ion batteries. *J Power Sources* 1997;**68**:195–200.
15. Dahn JR, Wilson AM, Xing W, Zank GA, inventors. Dow Corning Corp., assignee. Electrodes for lithium ion batteries using polysilanes. United States patent US 6,306,541(B1); 2001 Oct 23.
16. Dahn JR, Eguchi K, Wilson AM, Xing W, Zank GA, inventors. Dow Corning Corp., assignee. Electrodes for lithium ion batteries using polysiloxanes. United States patent US 5,824,280(A); 1998 Oct 20.
17. Ahn D, Raj R. Thermodynamic measurements pertaining to the hysteretic intercalation of lithium in polymer-derived silicon oxycarbide. *J Power Sources* 2010;**195**:3900–6.

18. Sanchez-Jimenez PE, Raj R. Lithium insertion in polymer-derived silicon oxycarbide ceramics. *J Am Ceram Soc* 2010;**93**:1127–35.
19. Dahn JR, Wilson AM, Xing W, Zank GA, inventors. Dow Corning Corp., assignee. Electrodes for lithium ion batteries using polysilazanes ceramic with lithium. United States patent US 5,631,106(A); 1997 May 20.
20. Kolb R, Fasel C, Liebau-Kunzmann V, Riedel R. SiCN/C-ceramic composite as anode material for lithium ion batteries. *J Eur Ceram Soc* 2006;**26**:3903–8.
21. Graczyk-Zajac M, Fasel C, Cherkashihnin G, Jaegermann W, Riedel R. Novel graphite/SiCN negative electrode materials for lithium-ion batteries with enhanced capacity and rate capability. In: *Lithium Battery Discussion Workshop 2009 – Electrode Materials*. 2009.
22. Su D, Li Y-L, Feng Y, Jin J. Electrochemical properties of polymer-derived SiCN materials as the anode in lithium ion batteries. *J Am Ceram Soc* 2009;**92**:2962–8.
23. Mera G, Riedel R, Poli F, Müller K. Carbon-rich SiCN ceramics derived from phenyl-containing poly(silylcarbodiimides). *J Eur Ceram Soc* 2009;**29**:2873–83.
24. Franklin RE. Crystallite growth in graphitising and non-graphitising carbons. *Proc R Soc Lond A* 1951;**209**:196–218.
25. Zheng T, Xue JS, Dahn JR. Lithium insertion in hydrogen-containing carbonaceous materials. *Chem Mater* 1996;**8**:389–93.
26. Zheng T, Dahn JR. Effect of turbostratic disorder on the staging phase diagram of lithium-intercalated graphitic carbon hosts. *Phys Rev B* 1996;**53**:3061–71.
27. Winter M, Appel WK, Evers B, Hodal T, Möller KC, Schneider I, et al. Studies on the anode/electrolyte interfacein lithium ion batteries. *Monatshefte für Chemie* 2001;**132**:473–86.
28. Gnanaraj JS, Levi MD, Levi E, Salitra G, Aurbach D, Fischer JE, et al. Comparison between the electrochemical behavior of disordered carbons and graphite electrodes in connection with their structure. *J Electrochem Soc* 2001;**48**:A525–36.
29. Larcher D, Mudalige C, George AE, Porter V, Gharghour M, Dahn JR. Si-containing disordered carbons prepared by pyrolysis of pitch/polysilane blends: effect of oxygen and sulfur. *Solid State Ionics* 1999;**122**:71–83.
30. Azuma H, Imoto H, Yamada S, Sekai K. Advanced carbon anode materials for lithium ion cells. *J Power Sources* 1999;**81-82**:1–7.
31. Zheng T, Liu Y, Fuller EW, Tseng S, von Sacken U, Dahn JR. Lithium insertion in high capacity carbonaceous materials. *J Electrochem Soc* 1995;**142**:2581–90.
32. Mera G, Tamayo A, Nguyen H, Sen S, Riedel R. Nanodomain structure of carbon-rich silicon carbonitride polymer-derived ceramics. *J Am Ceram Soc* 2010;**93**:1169–75.
33. Ferrari AC, Robertson J. Interpretation of Raman spectra of disordered and amorphous carbon. *J Phys Rev B* 2000;**61**:14095–107.
34. Wilson AM, Xing W, Zank G, Yates B, Dahn JR. Pyrolysed pitch-polysilane blends for use as anode materials in lithium ion batteries II: the effect of oxygen. *Solid State Ionics* 1997;**100**:259–66.
35. Martin-Gil M, Rabanal ME, Varez A, Kuhn A, Garcia-Alvarado F. Mechanical grinding of $Si_3N_4$ to be used as an electrode in lithium batteries. *Mater Lett* 2003;**57**:3063–9.